ELSEVIER

Journal of Photochemistry and Photobiology A: Chemistry 123 (1999) 99–108

Journal of Photochemistry and Photobiology A:Chemistry

Photochemistry and photophysics of donor-acceptor-polyenes. I: *all-trans*-4-dimethylamino-4′-cyano-1,4-diphenylbutadiene (DCB)

Heide Braatz[a], Stefan Hecht[b], Holger Seifert[a], Siegrun Helm[b], Jürgen Bendig[b,*], Wolfgang Rettig[1,a]

[a]*Institut für Chemie der Humboldt-Univ. Berlin, Physikalische und Theoretische Chemie, Bunsenstr. 1, D-10117 Berlin, Germany*
[b]*Institut für Chemie der Humboldt-Univ. Berlin, Organische Chemie, Hessische Straße 1-2, D-10115 Berlin, Germany*

Received 22 October 1998; accepted 25 January 1999

Abstract

Dimethylamino-cyano-diphenylbutadiene (DCB) has been investigated using photochemical and photophysical techniques. HPLC analysis enabled the separation of two photoisomers. Their absorption spectra and extinction coefficients were determined by combining the diode array spectra with the isosbestic points observed in photolysis. The forward and backward quantum yields of photoisomerization were determined. The quantum-chemical modelling of these spectra allowed for a tentative assignment of the photoisomers to the mono-*cis* isomers ct and tc. Fluorescence lifetimes and quantum yields allowed the conclusion of a negative solvatokinetic behaviour of the nonradiative decay. Catalyzed thermal isomerization of DCB was observed on reversed-phase chromatographic material.

Keywords: Photochemistry; Fluorescence; Polyenes; Diphenylbutadiene; Donor-acceptor; Catalysis

1. Introduction

Stilbenes are one of the photochemically and photophysically most studied compound families [1–3]. Photochemical *trans–cis* isomerization occurs in *trans*-stilbene after crossing a small activation barrier with the consequence that the reaction is sufficiently slowed down such that significant fluorescence is observable. For the reverse *cis–trans* photoisomerization, this barrier is very small such that the reaction becomes extremely fast, and the fluorescence is virtually absent. In recent years, the nature of the barrier along the *trans–cis* isomerization pathway has been a subject of controversy [4–6]. The barrier height has been shown to be medium dependent and to decrease with an increase of solvent density (pressure) in nonpolar solvents [7]. The barrier height changes reflect on the fluorescence quantum yields. Fluorescence quantum yields of *trans*-stilbene have also been reported to be solvent-polarity dependent [8]. The observed decrease of the fluorescence quantum yields with increasing solvent polarity can be understood within the model of 'sudden polarization' [9] or biradicaloid states [10] as indicating the polar nature of the double-bond twisted excited intermediate ('phantom-singlet-state' P^*). Highly polar solvents energetically lower P^* more strongly than the nonpolar precursor state E^*, such that the barrier between E^* and P* has to decrease.

In donor–acceptor(DA)-substituted stilbenes, the solvent polarity exerts the opposite effect, i.e., fluorescence lifetimes and quantum yields increase with increasing solvent polarity. This is not only observed for true stilbenes, e.g., substituted with dimethylamino- and cyano-substituents [11], but also for stilbenoid-type dyes of large practical importance such as the laser dye DCM [11], which consequently performs well only in highly polar solvents like DMSO [12,13]. Similarly to the non-substituted stilbene, this behaviour can be understood within the model of biradicaloid states, because in DA-stilbenes, the nature of P^* is expected to reverse to a weakly polar 'dot–dot structure' [14–16], whereas the precursor state E^* becomes highly polar due to strong mesomeric interaction in the planar conformation [15,16]. The source for the dependence of fluorescence quantum yields and lifetimes on solvent polarity is, thus, the differently polar nature of precursor and product states and its influence on the reaction kinetics via changes of barrier height or position. This has been termed solvatokinetic dependence [17]: a positive solvatokinetic dependence (reaction rate constants increasing with solvent polarity) is

*Corresponding author.
[1]Also corresponding author.

1010-6030/99/$ – see front matter
PII: S1010-6030(99)00024-6

indicative of a product more polar than the precursor, and vice versa for a negative solvatokinetic dependence.

DA-stilbenes like dimethylamino-cyano-stilbene (DCS) not only show relatively large fluorescence quantum yields in highly polar solvents due to their negative solvatokinetic behaviour but also because the activation barrier is enlarged due to a different source. This source seems to be linked to the twisting possibility around the single bonds adjacent to the double bond. For a doubly bridged compound, where both these single bonds are rigidly held in the planar conformation, the reaction barriers under isolated-molecule conditions in the supersonic jet are virtually absent but sizable for DCS with flexible phenyl groups [18]. This difference in barrier height is probably linked with the population of a third state A^* in solution which emits an additional fluorescence band at very short times [19,20] and which has been connected with the well-known twisted intramolecular charge transfer (TICT) states [16,21,22], because A^* is neither populated in weakly polar solvents [23,24] nor in single-bond bridged model compounds [23] and, hence, has charge transfer nature and necessitates intramolecular twisting. This twisting is probably only partial and does not necessitate the fully perpendicular structure, because A^* possesses allowed emissive properties [23] consistent with a large coupling between the subunits.

Proceeding to the higher members of DA-diphenyl-polyenes, we focus here on dimethylamino-cyano-diphenylbutadiene (DCB) and the question whether a similar negative solvatokinetic dependence as in DCS is observed and try to get some indication whether excited-state barriers are present in the *all-trans* and the mono-*cis* conformations. For this purpose, we isolated the photoisomers and determined their absorption and their qualitative fluorescence properties as well as their quantum yields. Since DCB has two different substituents, it can form two different mono-*cis* isomers, unlike the symmetric diphenylbutadiene with only one *cis*-isomer [25,26]. Moreover, the question of whether low-lying ^1A_g states are important has to be dealt with. ^1A_g states are known to produce the anomalously long fluorescence lifetimes and high quantum yields in diphenylpolyenes [27–31].

A final question concerns the thermal isomerization. The *cis*-isomers being thermodynamically less-stable than the *trans*-isomers, the former would convert thermally to the *trans*-isomers for sufficiently small ground state activation barriers. Experimentally, *cis*-stilbenes are stable under thermal conditions, but related compounds such as aza-derivatives show thermal *cis–trans* isomerization with a rate constant depending on solvent polarity [32]. Similarly as for the excited state, a positive or negative solvatokinetic behaviour can be discerned for the ground state isomerization [16]. Ground- and excited-state behaviour can be combined within the biradicaloid model leading to the prediction that a negative excited-state solvatokinetic behaviour is linked with a positive one in the ground state and vice versa. This has been termed the 'Yin-Yang' principle [16] and allows to predict the electronic structure at the top of the ground state activation barrier. For compounds with negative solvatokinetic behaviour in the excited state, like DCS, the barrier is predicted to correspond to a highly dipolar structure. Medium effects, e.g., on highly polar surfaces might be able to lower this barrier sufficiently such that thermal isomerization even in stilbenes becomes possible. This would enable a new approach in the understanding of heterogeneous catalysis of double-bond isomerizations. Here, we report on the thermal *cis–trans* isomerization of *cis*-DCB induced by catalytic interaction with a reversed-phase chromatographic material.

2. Experimental and calculations

2.1. Materials

2.1.1. Solvents

All organic solvents used for spectroscopy were Uvasol grade from Merck. Water was triply distilled.

Synthesis of trans, trans-4-cyano-4′-dimethylamino-1,4-diphenyl-1,3-butadiene (t): The chemicals were used as purchased from Aldrich Chemical Company. All preparations and investigations were carried out under yellow light.

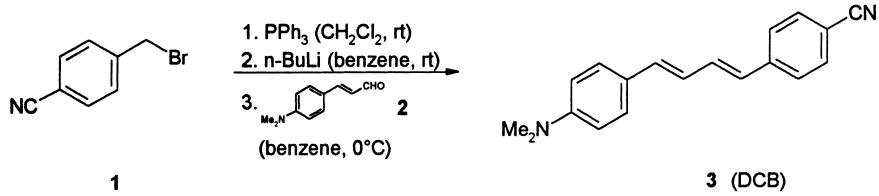

A solution of 0.98 g (5 mmol) 4-cyanobenzyl bromide **1** (Aldrich) and 1.31 g (5 mmol) triphenylphosphine in 30 ml methylene chloride was stirred at room temperature for 18 h. The white precipitate formed was filtrated, washed thoroughly with ether, and yielded the desired phosphonium salt in almost quantitative yield (98%).

3.1 ml of 1.6 M n-butyl lithium (4.9 mmol) were added to a suspension of 2.25 g (4.9 mmol) 4-cyanobenzyl triphenylphosphonium bromide in 20 ml benzene and stirred for 15 min. The mixture was cooled to 0°C (ice bath). A suspension of 0.86 g (4.9 mmol) 4-dimethylamino cinna-

monaldehyde **2** in 30 ml benzene was slowly added and stirring was continued at room temperature for another 18 h.

The crude reaction mixture was quenched with sodium bicarbonate/water, extracted with methylene chloride, the collected phases were washed with water and dried over magnesium sulfate. The solvent was evaporated, the residue taken up in 2 M hydrochloric acid, extracted with ether, and the inorganic layer brought back to a pH = 10 with sodium carbonate. The orange precipitate formed was filtrated and recrystallized from ethanol to yield 0.4 g (1.5 mmol) DCB **3** (30% overall yield).^{1}H-NMR ($CDCl_3$): δ 2.97 (6H, s), 6.56 (1H, d, $J = 15.1$ Hz), 6.66 (1H, d, $J = 15$ Hz), 6.67 (2H, d, $J = 8.7$ Hz), 6.78 (1H, dd, $J = 15.4$, 10.2 Hz), 7.03 (1H, dd, $J = 15.4$, 10.2 Hz), 7.33 (2H, d, $J = 8.7$ Hz), 7.44 (2H, d, $J = 8.3$), 7.88 (2H, d, $J = 8.3$ Hz), ^{13}C-NMR ($CDCl_3$): δ 38.2, 40.4, 112.3, 124.6, 125.9, 127.8, 128.6, 132.8, 135.2 UV (EtOH): λ_{max} 407, 307 nm; (MeOH/water, 75 : 25): $\lambda_{max}(\epsilon_{max})$ 399(42000 l mol^{-1} cm^{-1}) IR (KBr): 3417, 3011, 2220, 1587, 1520, 1357, 990 cm^{-1}

2.2. Instrumentation

^{1}H and ^{13}C NMR spectra were recorded using an AV 300 (Bruker). UV spectra were recorded using a UVICON 930 (Kontron Instruments) and a U-3410 (Hitachi) spectrometer.

HPLC was carried out using the following conditions: Kontron HPLC pump 422, Knauer injection valve with 20 μl sample loop; mobile phase, methanol–water (75 : 25); flow rate 0.5 ml min^{-1}; Knauer column (250 mm x 4 mm) filled with LiChrosorb RP 18 (5 μm); diode array detector Kontron DAD 44O.

2.3. Fluorescence and quantum yield measurements

Fluorescence spectra were recorded on an SLM Aminco Bowman AB2 fluorescence spectrometer and corrected for instrument response and dependence excitation energy. The emission correction curves were created using a calibrated tungsten lamp from SLM Instruments (Emission correction kit FP-123). The excitation correction curves were created using the excitation spectrum of a quantum counter solution of Basic Blue 3 with a concentration of 4.1 g l^{-1} [33]. The emission corrected spectra were divided by the intensity values of this spectrum at the excitation wavelengths. For the determination of the fluorescence quantum yields the optical densities of the solutions were measured with a Unicam UV 4 absorption spectrometer. Quinine bisulphate in 0.1 N H_2SO_4 ($\Phi_f = 0.515$ [34]) and Rhodamin 101 in ethanol ($\Phi_f = 1.0$ [35]) were used as fluorescence standards. The solutions of DCB were prepared under red light and were not degassed.

There are two complications with respect to the determination of the fluorescence quantum yield for compounds such as **t-DCB** showing strong photoisomerization reactions: (i) the fluorescence intensity diminishes during the measurement of the fluorescence spectrum due to the disappearance of the *trans*-isomer; (ii) the total optical density diminishes because the *cis*-isomers exhibit a smaller extinction coefficient than the *trans*-isomer. When the fluorescence spectrum is recorded with a slow scan speed in order to obtain a good signal-to-noise ratio both effects falsify the value of the fluorescence quantum yield in a manner which cannot be corrected. In order to avoid these distortions of the fluorescence quantum yields by *trans→cis* photoisomerization and to measure the fluorescence spectrum under stable and reproducible conditions we chose a modified measurement technique.

At the maximum wavelength of the fluorescence spectrum a time trace of the subsiding intensity is recorded until the photostationary state of the solution is safely reached. The fluorescence spectrum is then recorded in the photostationary state with a slow scan speed and the intensity is scaled to the value at time $t = 0$ using the time trace (Fig. 1(a)). During the whole measurement time the solution is intensively stirred. The resulting spectra are shown in Fig. 1(b) for diethylether and ethanol solvents.

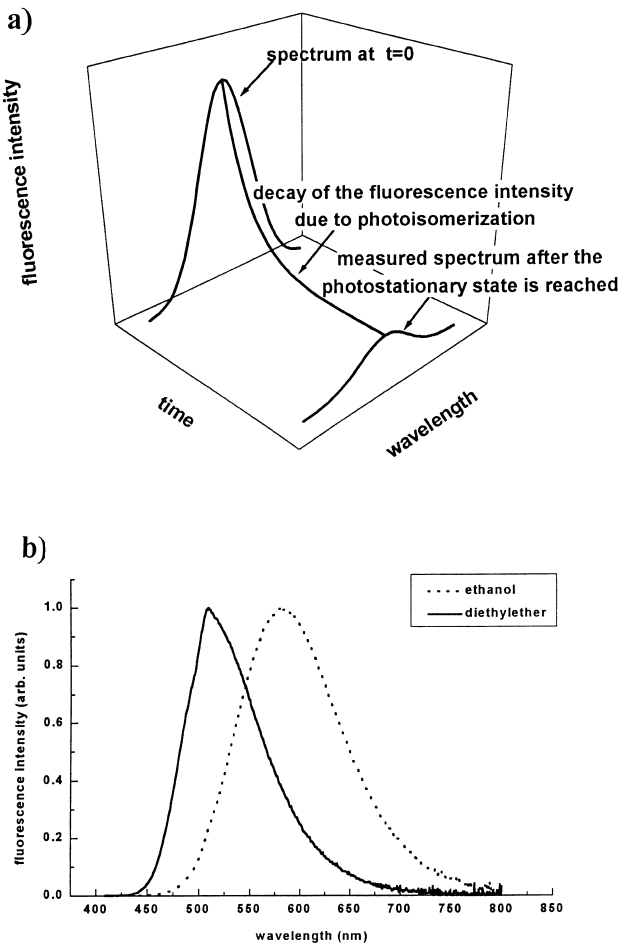

Fig. 1. (a) Principle of the measurement method used for the determination of fluorescence quantum yields of compounds showing photoisomerization. (b) Fluorescence spectrum of DCB in ethanol and diethylether constructed by combining 30 spectra, respectively, in the manner described in the text.

The applicability of this method results from the absence of the fluorescence of the *cis*-isomers. This was checked with the following two experiments. First, the HPLC-separated isomer products were collected in sufficient quantity and the fluorescence spectra were measured. The *cis*-isomers did not show any detectable fluorescence. Second, the process of photoisomerization was monitored by the measurement of 100 fluorescence spectra with high scan speed before the photostationary state was reached. Analysis of these 100 spectra with the chemometrical method of singular value decomposition [36,37] which yields the number of independent fluorescent components showed that the set of spectra consisted of only one component, that of the fluorescence spectrum of the *trans*-isomer. If there would have been any detectable fluorescence originating from the *cis*-isomers it would have shown up as a second small component by the singular value decomposition. In the fluorescence spectrometer used it takes about 60 min until the photostationary state is reached for an *all-trans* DCB solution with a volume of 2 ml, optical densities between 0.1 and 0.2 and a bandpass of the excitation monochromator of 2 nm. The scan speed of 40 nm s^{-1} can be considered as fast compared with the time needed for completion of the photoisomerization, therefore, the individual fluorescence spectra recorded during the reaction are not distorted by the isomerization.

Fluorescence decay time measurements were performed using synchrotron radiation from BESSY in Berlin as excitation source. Details of the Time Correlated Single Photon Counting equipment used can be found in [38]. The time resolution achieved was about 100 ps.

3. Quantum chemical calculations and simulation of the absorption spectra

Ground state structures were optimized with the program package AMPAC 5.0 [39]. Absorption spectra were calculated using the CNDO/S framework[2] [40–42] and for the purpose of comparison also calculated with the configuration interaction (CI) routine implemented in AMPAC 5.0, which also includes higher excitations. The AM1 hamiltonian has been used both for ground state optimization and calculation of spectra with AMPAC 5.0. The optimized geometries were used for the calculation of the spectra with both programs. Within AMPAC 5.0 the CAS consisted of seven occupied and seven unoccupied molecular orbitals symmetrically distributed around the HOMO-LUMO transition. 312 microstates (configurations) were selected from the roughly 12 million microstates generated, according to the selection scheme implemented in the program package. We were able to use 312 instead of 100 microstates usually available with AMPAC 5.0 due to use of the undocumented keyword CIMAX [43]. For the CNDO/S–CI calculations, the 50 singly excited and the 50 doubly excited configurations lowest in energy were used.

For the comparison with the experimental spectra, every line calculated was broadened with a Gaussian normal distribution function of a standard deviation of 0.23 eV. All the Gaussian functions were added in order to simulate the absorption spectra in solution. For a better comparison with the measured spectra, the spectra calculated on a wavenumber scale with energy-independent widths were transformed into a wavelength scale. They are shown in Fig. 5 below. The total spectrum of one isomer consists of the sum of the spectra of the respective s-*trans* and the s-*cis* conformer according to their mole fractions $x_{\text{s-}trans}$, $x_{\text{s-}cis}$ calculated from the enthalpies of formation and the resulting equilibrium constant (Table 3). We have not included the influence of the entropy on the mole fractions and on K for the following reason: test calculations including the entropy (keyword FORCE in AMPAC) indicated that the difference in the Gibbs free enthalpy of the s-*trans* and the s-*cis* conformer of the *all-trans*-isomer is 1.07 kcal mol^{-1}. From that the mole fractions are $x_{\text{s-}trans} = 0.86$ and $x_{\text{s-}cis} = 0.14$, i.e., very close to the values in Table 3 (0.81 and 0.19). The resulting shape of the total spectra is negligibly affected. Therefore, for the purpose of classification of the isomers the enthalpies produced by AMPAC 5.0 and the resulting equilibrium constants due to Table 3 can be directly used.

4. Photochemistry and reaction quantum yield measurements

Photolysis was carried out using a high-pressure mercury lamp (HBO 500, Oriel, USA) with controlled light intensity and a metal interference filter of 468 nm (Schott-Glaswerke, Germany). The irradiation spectra were recorded with a spectrometer (U-3410, Hitachi, Japan) combined with a computer and the software package SPECTRACALC. The irradiated solutions were analyzed using HPLC.

The quantum yields were determined as described in [44] using the potassium ferrioxalate actinometer [45]. The initial slope dc/dt of the experimentally obtained concentration/irradiation-time function was determined directly using the HPLC peak intensities. The value of the absorbed light intensity at $t = 0$ for the irradiation wavelength was taken from the UV/Vis spectra.

5. Thermal isomerization on reversed-phase chromatographic material

3 ml ethanolic solution of **t** were irradiated ($\lambda_{\text{exc}} = 436$ nm) to the photostationary state and then kept in the dark on 50 mg reversed-phase chromatographic material RP 18 (Polymer Laboratories, UK). The isomerization effect was monitored by UV/Vis spectra (see Fig. 7 below).

[2]QCPE program no. 333 with the original parameters has been used.

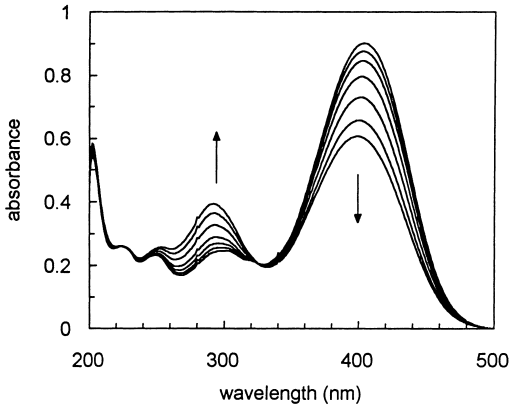

Fig. 2. Isosbestic points observed in the photolysis of *all-trans*-DCB (**t**) in (ethanol).

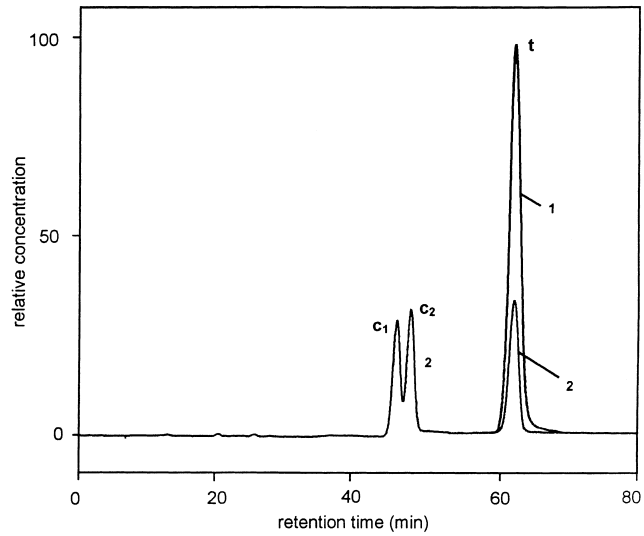

Fig. 3. HPLC-traces showing the separation of the photolysed mixture into the starting material (**t**) and the two photoisomers $\mathbf{c_1}$ and $\mathbf{c_2}$.

6. Results

The irradiation ($\lambda_{exc} = 468$ nm) of *trans,trans*-4-cyano-4′-dimethylamino-1,4-diphenyl-1,3-butadiene (**t**) in ethanol at room temperature leads to a decrease in absorption band intensity combined with a slight hypsochromic shift (Fig. 2). The reaction is uniform within the whole period of photolysis, which is demonstrated by an isosbestic point at 324 nm as well as by the linear ΔE diagram (not shown). The irradiated solution is stable in the dark at room temperature. The intensity of the final irradiation spectrum depends upon the excitation wavelength. At long wavelength excitation ($\lambda_{exc} = 486$ nm, 436 nm) the decrease is stronger than on short wavelength photolysis ($\lambda_{exc} = 365$ nm, 313 nm). This behaviour is an argument for the existence of photochemical equilibria with different isomer content depending upon the specific absorption properties of the isomers involved as described by Zimmerman et al. [46].

The formation of two isomers ($\mathbf{c_1}$ and $\mathbf{c_2}$) as well as the remaining **t** during the course of photolysis was observed using HPLC (Fig. 3). Compared with the *all-trans* isomer the photoproducts appear at shorter retention time. The ratio of the peak intensities of $\mathbf{c_1}$ and $\mathbf{c_2}$ is constant within the whole period of photolysis. Using the diode array detector the relative (non-scaled) absorption spectra of both photoisomers have been measured (the spectra on an absolute scale are shown in Fig. 5).

The kinetic behaviour of both the irradiation spectra and the HPLC peak intensities of the isomers are in agreement with the parallel reaction schemes (1) and (2).

$$\mathbf{t} \xrightarrow{h\nu} \mathbf{c_1} \tag{1}$$

$$\mathbf{t} \xrightarrow{h\nu} \mathbf{c_2} \tag{2}$$

For the irradiation of the photoproducts $\mathbf{c_1}$ and $\mathbf{c_2}$, the photolyzed solution of **t** (shown in Fig. 2) was separated repeatedly ten times using HPLC and the obtained fractions of $\mathbf{c_1}$ and $\mathbf{c_2}$ were collected, respectively. The irradiation spectra of the photochemical reconversion are shown in Fig. 4(a) ($\mathbf{c_1}$) and Fig. 4(b) ($\mathbf{c_2}$). Both reactions are uniform only within the initial period of photolysis, and only these initial irradiation spectra are shown in Fig. 4(a) and Fig. 4(b). Further photolysis, not shown in these figures, leads to the disappearance of the isosbestic points at 334 nm ($\mathbf{c_1}$) and 298 nm ($\mathbf{c_2}$). Within the initial period of photolysis, only the formation of **t** is observed. This means the spectra in Fig. 4(a) represent the photoreaction (3) and those in Fig. 4(b) belong to the photoreaction (4).

$$c_1 \xrightarrow{h\nu} t \tag{3}$$

$$c_2 \xrightarrow{h\nu} t \tag{4}$$

Generally, the existence of an isosbestic point in the irradiation spectra of an A → B reaction is caused by the fact that the molar absorption coefficients of both species involved are identical [47]. For DCB, the molar absorption coefficients of **t** and $\mathbf{c_1}$ are identical at $\lambda = 334$ nm and the species **t** and $\mathbf{c_2}$ have the same values of ε at $\lambda = 298$ nm. On the basis of the known absorption coefficients of **t** at the isosbestic wavelengths the scaling of the relative spectra of $\mathbf{c_1}$ and $\mathbf{c_2}$ (from the diode array detector) was carried out (Fig. 5).

The concentration/time dependence of the species involved **t**, $\mathbf{c_1}$ and $\mathbf{c_2}$ is shown in Fig. 6 by the corresponding HPLC peak intensities. The character of the curves is typical for the existence of a photochemical equilibrium. At the conditions used, after an exposure time of about 300 s, the photostationary state is reached. During irradiation the solution was stirred.

The initial slope of the curves both of the photolysis ($-\mathrm{d}c(\mathbf{t})/\mathrm{d}t$) and of the formation ($\mathrm{d}c(\mathbf{c_1})/\mathrm{d}t$, $\mathrm{d}c(\mathbf{c_2})/\mathrm{d}t$) allow

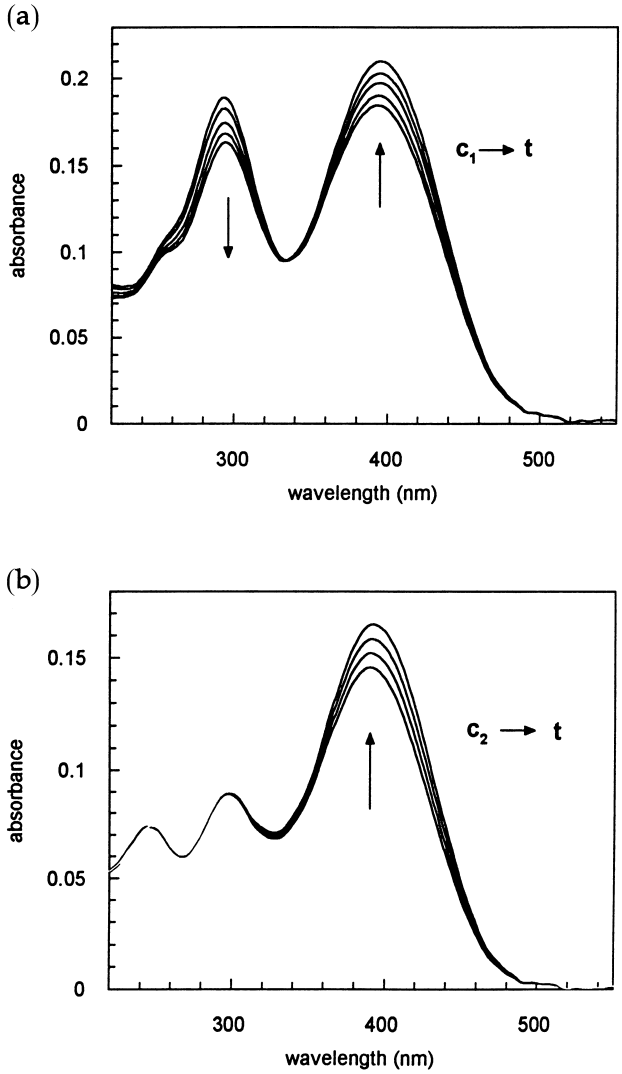

Fig. 4. Absorption spectra of the separated photoisomers $\mathbf{c_1}$ (a) and $\mathbf{c_2}$ (b) and their photochemical reconversion to **t** (MeOH : water = 75 : 25).

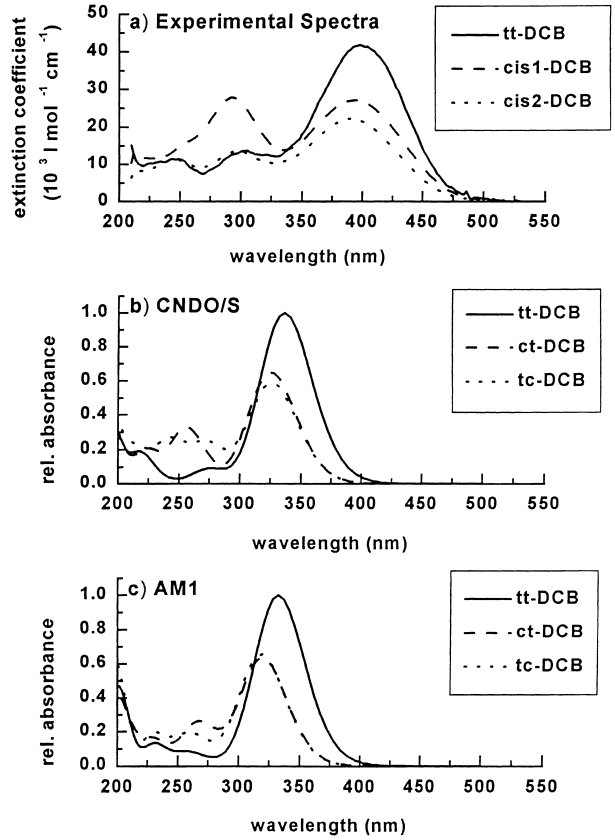

Fig. 5. Absorption spectra of *all-trans* (**t**) and the two *cis*-isomers $\mathbf{c_1}$ and $\mathbf{c_2}$ in MeOH : water = 75 : 25 on an absolute absorbance scale (a) and comparison of the spectral modelling using the CNDO/S-CI (b) and AM1-CI (c) methods.

the determination of the overall quantum yield $\varphi(\mathbf{t} \rightarrow \mathbf{c_1} + \mathbf{c_2})$ and the values for $\varphi(\mathbf{t} \rightarrow \mathbf{c_1})$ and $\varphi(\mathbf{t} \rightarrow \mathbf{c_2})$ by comparison with the ferrioxalate actinometer (Table 1). Starting from the electronically excited state $\mathbf{t}^*$ the formation of the $\mathbf{c_2}$ isomer is favoured (relative efficiency 0.60) compared with the competing isomer $\mathbf{c_1}$ (relative efficiency 0.40).

The quantum yields for the photochemical back reactions (3) and (4) are determined in the same manner using the initial slope of the concentration/time functions of the irradiation of the separated isomers $\mathbf{c_1}$ and $\mathbf{c_2}$ (Fig. 4(a,b) by the relative method. The isomer $\mathbf{c_2}$ shows a slightly higher photoreactivity than $\mathbf{c_1}$ (Table 1).

At room temperature and in the dark, the isomers $\mathbf{c_1}$ and $\mathbf{c_2}$ in solution (ethanol, hexane) are stable, the change of the absorbance is less than 2% within 10 days. A significant thermal isomerization is not observed until 80°C. Quite different from that, upon contact with alkylsilylated silica gel (a common reversed phase material RP18 used in chromatography) a thermal back reaction of the photochemically generated mixture of the isomers is observed (Fig. 7). The rate of this catalytical isomerization is independent of the concentration of DCB dissolved with respect to the amount of RP 18 material added.

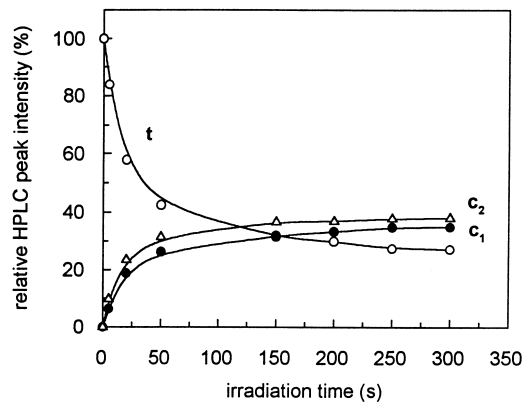

Fig. 6. Relative HPLC peak intensities of **t**, $\mathbf{c_1}$ and $\mathbf{c_2}$ depending on the irradiation time (ethanol, $\lambda_{exc} = 436$ nm)

Table 1
Absorption spectral data of the separated *trans*- (**t**) and *cis*-isomers ($\mathbf{c_1}$, $\mathbf{c_2}$) of DCB, composition of the photostationary equilibrium and reaction quantum yields.

	t	$\mathbf{c_1}$	$\mathbf{c_2}$
λ_{max}[a] (nm)	399/305/252	395/293/254(sh)	390/298/245
ε_{max}[a] (l mol^{-1} cm^{-1})	42,000/13,550/11,320	27,550/28,500/15,760	21,790/13,330/11,110
	$\mathbf{t}^* \rightarrow \mathbf{c_1} + \mathbf{c_2}$	$\mathbf{c_1}^* \rightarrow$ t	$\mathbf{c_2}^* \rightarrow \mathbf{t}$
Isosbestic point (nm)	325[b], 324[a]	334[a]	298[a]
Photostationary equilibrium[c]	26% **t**		
	34% $\mathbf{c_1}$		
	40% $\mathbf{c_2}$		
Quantum yields[a]	$\varphi(\mathbf{t} \rightarrow \mathbf{c_1} + \mathbf{c_2}) = 0.30$		
	$\varphi(\mathbf{t} \rightarrow \mathbf{c_1}) = 0.12$		
	$\varphi(\mathbf{t} \rightarrow \mathbf{c_2}) = 0.18$		
		$\varphi\ (\mathbf{c_1} \rightarrow \mathbf{t}) = 0.42$	
			$\varphi(\mathbf{c_2} \rightarrow \mathbf{t}) = 0.46$

[a] MeOH : water (75 : 25).
[b] Ethanol.
[c] $\lambda_{exc} = 436$ nm.

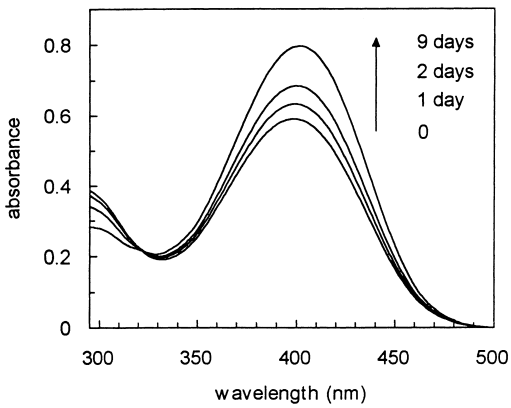

Fig. 7. Thermal isomerization (dark reaction) on RP phase starting from the photostationary state in ethanol.

7. Discussion

7.1. Solvatokinetic behaviour and decay to the ground state

The fluorescence quantum yield and lifetime values in Table 5 display a characteristic solvent dependence: quantum yields are higher and lifetimes longer in the more polar solvent. A similar observation has been made for the shorter chain analogue DCS [11,48] and several other donor–acceptor stilbenes. The main effect can be seen in a decrease of the nonradiative decay rate constants. The latter is mainly due to the photochemical *trans–cis* reaction which is, therefore, slowed down in more polar solvents (negative solvatokinetic behaviour). The opposite effect is observed for stilbene without donor–acceptor substituents [1–3] and can be called positive solvatokinetic behaviour. An explanation for this opposing behaviour can be found in the theory of biradicaloid states [10,14–16]: it rests upon the solvent influence on the energies of precursor and product states of the photochemical reaction. In stilbene, the primary excited precursor state E^* is nonpolar, yet the product of the adiabatic photoreaction, the double-bond twisted phantom singlet state P^* (tentatively to be identified with a conical intersection or photochemical funnel) is highly polar [8] and hence more strongly stabilized by polar solvents leading to a higher thermodynamic driving force and accelerated reaction rates. The theory of biradicaloid states predicts that P^* will change its nature to become weakly polar, if the donor and acceptor substituents are strong enough [10,14–16]. On the other hand, E^* gains polar character, and the situation reverses to a highly polar E^* and a weakly polar P^* state which cause negative solvatokinetic behaviour as observed in the experiment and independently verified by quantum chemical calculations [8]. The parallel behaviour of DCB, therefore, leads to the conclusion that the photochemical funnel in this case is also weakly polar and has a so-called dot–dot structure [10,16] with an odd electron on each moiety adjacent to the twisted double bond.

A further interesting conclusion can be drawn by comparison of the nonradiative decay rate of DCB (0.3–0.5 ns^{-1}) to that of butadiene where the decay occurs on the femtosecond timescale [49]. Therefore, the kinetics of DCB is nearly 1000 times slower than that of butadiene. A possible clue to this astonishingly large factor is that the decay of butadiene occurs on a barrierless potential through a conical intersection involving several twisted bonds [49,50]. In the case of DCB, larger groups are involved in this large-amplitude relaxation process, and an energetic barrier is likely to separate the fluorescing state from the conical intersection. The reason is the possibility for an additional relaxation process for donor–acceptor diphenylethylene, -buta-diene and -hexatriene, starting from E^*, namely the formation of a charge transfer state A^* or of several different ones. This has been demonstrated in the case of DCS to necessitate a large-amplitude twisting

motion around one of the single bonds, most probably of the dimethylanilino moiety [23]. This relaxation $E^* \rightarrow A^*$ competes with the $E^* \rightarrow P^*$ decay and leads to dual fluorescence for DCS and multiple fluorescence for DCB and the hexatriene derivative on the timescale of a few picoseconds [19,20,51,52]. It can, therefore, not be resolved with our present subnanosecond equipment but nevertheless has important photophysical consequences: since A^* is a CT state, its formation leads energetically downhill in polar solvents, and access to the conical intersection P^* has to overcome the activation barrier to E^*, if a simplified two-dimensional model [53] is used for discussion. This activation barrier can be expected to be one of the main sources slowing down the rate of the photochemical reaction in DCB.

7.2. Photochemistry

The kinetic analysis of both the irradiation spectra (Fig. 1, Fig. 3(a) and Fig. 3(b)) and the relative concentration of the involved species determined using HPLC (Fig. 2) prove the parallel photoisomerization of **t** forming $\mathbf{c_1}$ and $\mathbf{c_2}$. The UV/Vis spectra of $\mathbf{c_1}$ and $\mathbf{c_2}$ are blue shifted and of weaker oscillator strength in the long wavelength region (Fig. 4). The differences in the UV/Vis spectroscopic properties of **t** on the one hand and $\mathbf{c_1}$ and $\mathbf{c_2}$ on the other hand are very similar to those of the *trans,trans*- and *cis,trans*-isomer of 1,4-diphenylbutadiene [54]. Therefore, we conclude that $\mathbf{c_1}$ and $\mathbf{c_2}$ are the isomers of DCB which contain one *cis* double bond.

In the HPLC analysis of an irradiated solution (e.g., photostationary state) using RP material the *cis*-isomers appear at shorter retention time (Fig. 2), very similar to the stilbenes and to 1,4-diphenylbutadiene [55]. The (small) difference in polarity of $\mathbf{c_1}$ and $\mathbf{c_2}$, caused by the assymetric molecular structure, is the reason for the slight difference in the retention time of $\mathbf{c_1}$ and $\mathbf{c_2}$, $\mathbf{c_1}$ is more polar than $\mathbf{c_2}$.

Utilizing the different retention times the separation of $\mathbf{c_1}$ and $\mathbf{c_2}$ in dilute solutions is successful. Upon irradiation of the separated pure solutions of $\mathbf{c_1}$ and $\mathbf{c_2}$, respectively, an initial phase corresponding to a pure $A \rightarrow B$ reaction is observed, characterized by the existence of isosbestic points and linear ED diagrams [56]. The change in the UV/Vis spectra (Fig. 3(a,b)) indicates the formation of **t**. Only upon prolonged photolysis the formation of $\mathbf{c_2}$ (starting from c_1) and $\mathbf{c_1}$ (starting from $\mathbf{c_2}$) is observed. A direct pathway of photoisomerization starting from a single excited state of $\mathbf{c_1}$ and $\mathbf{c_2}$ forming $\mathbf{c_2}$ and $\mathbf{c_1}$, respectively, does not occur.

The chromatographic separation of the isomers $\mathbf{c_1}$ and $\mathbf{c_2}$ is successful only for dilute solutions ($c < 10^{-3}$ M). The preparation of the sufficiently pure isomers $\mathbf{c_1}$ and $\mathbf{c_2}$ in the milligram scale using preparative HPLC was not possible. Therefore, no NMR spectra could be taken, and the relation of $\mathbf{c_1}$ and $\mathbf{c_2}$ to the *trans,cis*- or *cis,trans*-configuration could not be established.

At room temperature, the formation of a further product, the possible *cis,cis*-isomer was not observed.

7.3. A possible assignment of the photoisomers

In view of the difficulties in assigning the photoisomers by NMR spectroscopy, quantum-chemical modelling calculations have been applied (Tables 2–5). These can predict both thermodynamic and structural factors influencing the spectra of isomers and the population of possible conformers.

Table 2
Heats of formation and structural parameters of various optimized ground state conformers and isomers of DCB. For the numbering of the dihedral angles see the structure below

Central single bond	Double bonds		$\Delta_B H$	Dihedral angles in the polyene chain				
	1	2	kcal mol^{-1}	φ_1	φ_2	φ_3	φ_4	φ_5
Trans	*Trans*	*Trans*	113.37	−11.02	179.98	−179.45	179.90	18.95
	Cis	*Trans*	115.16	42.34	3.00	−168.25	179.26	20.50
	Trans	*Cis*	115.06	14.78	−179.30	−169.50	2.54	43.91
Cis	*Trans*	*Trans*	114.23	15.69	179.92	18.08	179.83	21.62
	Cis	*Trans*	117.60	−40.11	−3.28	-35.97	−177.43	17.55
	Trans	*Cis*	117.50	-8.97	177.42	37.42	2.86	40.22

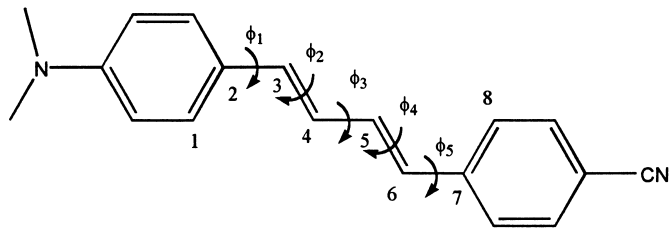

Definition of the dihedral angles printed in Table 2: ϕ_1 corresponds to the dihedral angle defined by atoms 1–4, etc.

Table 3
Heats of formation $\Delta_B H$, and their difference $\Delta(\Delta_B H)$, equilibrium constants K, and mole fractions $x_{s\text{-}trans}$ and $x_{s\text{-}cis}$ used for the simulation of the spectra for the respective conformers of the three isomers of DCB

	s-*trans*-conformer $\Delta_B H$ (kcal mol^{-1})	s-*cis*-conformer $\Delta_B H$ (kcal mol^{-1})	$\Delta(\Delta_B H)$ (kcal mol^{-1})	K	$x_{s\text{-}trans}$	$x_{s\text{-}cis}$
tt-isomer	113.37	114.23	0.86	0.234	0.810	0.190
ct-isomer	115.16	117.60	2.44	0.016	0.984	0.016
tc-isomer	115.06	117.50	2.44	0.016	0.984	0.016

Table 4
Results of the spectral fitting: relative extinction coefficients at the wavelength of the total maximum and the maximum of the '*cis*'-peak. The values in the columns 'maximum' are relative to the calculated extinction coefficient of the *all-trans* isomer, the values in the columns '*cis*-peak' are relative to the maximum extinction coefficient of the respective isomer

	CNDO/S				AM1, CI = 14, CIMAX = 400			
	Maximum		'*Cis*'-peak		Maximum		'*Cis*'-peak	
	λ	$\varepsilon(\lambda_{max})$	λ	ε_{rel}	λ	$\varepsilon(\lambda_{max})$	λ	ε_{rel}
tt	336.9	1.00	276.8	0.09	336.9	1.00	256.7	0.09
ct	323.7	0.65	256.7	0.51	319.6	0.64	267.8	0.42
tc	328.0	0.59	270.7	0.43	319.6	0.66	259.4	0.30

Regarding the rotation around the single bonds in DCB, these require little activation energy in the ground state and occur thermally. It is, therefore, important to know the relative abundance of s-*cis*, s-*trans* conformers (which differ in the *cis*- or *trans*-arrangement regarding the central single bond ϕ_3, whereas rotation around the terminal single bonds ϕ_1 and ϕ_5 leads to identical products). The calculations predict an equilibrium energy difference <1 kcal mol^{-1} for the *trans,trans*-isomer and hence a significant population of s-*cis* at room temperature (Table 3). In the case of the *cis,trans*- and *trans,cis*-isomer, these energy differences are larger (ca 2.5 kcal mol^{-1}), and the population of the s-*cis* conformer can be neglected.

The terminal phenyl groups are only slightly twisted in the *trans,trans*-isomer (10–20°) whereas in the sterically more crowded mono-*cis* isomers *cis,trans* and *trans,cis*, one of the phenyl rings is twisted to around 40° (the one close to the *cis*-bond). For the *cis,trans*-isomer with double bond 1 (corresponding to bond 3-4 in the formula of Table 2) in the *cis*-arrangement, the anilino group will be more strongly twisted, whereas for the *trans,cis*-isomer, the benzonitrile group is the more twisted one (Table 2). This additional twist of one of the phenyl groups leads to a blue shift of spectra and a reduction of the oscillator strength as evidenced by the results of excited-state calculations (Table 4). As it turns out, this effect is predicted to be rather similar for the long wavelength band of both isomers (Table 4 and Fig. 5(b,c)), in accordance with the experimental results (Fig. 5(a)), although the calculated spectra are somewhat blueshifted with respect to the experimental ones, which is a general observation for this type of donor–acceptor compounds [57]. The strongest difference between the two experimental *cis*-isomers is the relative intensity of their '*cis*-peak' around 300 nm which is especially pronounced for **c$_1$**-DCB, i.e., the isomer appearing first in the HPLC analysis. By comparison with the relative intensity of the corresponding band of the calculated spectra at around 250 nm, we tentatively assign **c$_1$** to the isomer *cis,trans*-DCB, i.e., the mono-*cis*-isomer where the anilino group is more strongly twisted.

7.4. Catalyzed thermal isomerization and the Yin-Yang model

Under normal conditions, substituted stilbenes, butadienes etc. are highly stable thermally, i.e., their activation barrier to *cis–trans* or *trans–cis*-isomerization is sufficient to suppress this reaction in the ground state. Only aza-derivatives (e.g., azobenzene or Schiff bases) are known to show thermal *cis–trans* isomerization. We reported above on the unusual observation of a thermal isomerization of DCB, under the catalytic influence of the reversed phase material.

A possible explanation can be found in terms of the so-called 'Yin-Yang model' [16]: this model applies to the

Table 5
Fluorescence quantum yields, lifetimes and derived photophysical rate constants of DCB in ethanol and ethyl ether at 298 K

Solvent	Φ_f	τ_f (ns)	k_f (ns^{-1})	k_{nr} (ns^{-1})
Diethyl ether	0.09	0.32	0.28	2.84
Ethanol	0.18	0.45	0.40	1.82

double-bond twisted situation of an ethylene derivative like stilbene, or a polyene, and links the excited-state properties with those of the ground state. For such an orbitally decoupled geometry, as it occurs in the funnel region and on the top of the ground state barrier, the excited and the ground state are expected to possess opposite dipolar properties. We concluded from the negative solvatokinetic behaviour of DCB that the excited state photochemical funnel possesses weakly dipolar properties. From the Yin-Yang model we can, therefore, infer a highly dipolar ground state barrier which should be strongly reduced in a sufficiently polar surrounding allowing for thermal isomerization.

The conjecture from this model is two-fold: (i) It allows to predict in which case it is possible to induce thermal isomerization around a C=C double bond, either based on experimental data refering to the excited state (fluorescence quantum yields or lifetimes) or from calculation of the electronic structure of the ground state. In general, catalyzed thermal isomerization should be possible for a sufficiently strong donor–acceptor substitution. (ii) It allows to understand which type of solute–catalyst interaction is important to bring down the activation energy. This understanding helps in devising new and more efficient catalysts.

Acknowledgements

We gratefully acknowledge the support through BESSY and the BMFT (project 05 414 SLT FAB9) as well as through the Deutsche Forschungsgemeinschaft which made the lifetime measurements possible. We also want to thank Dr. R. Lapouyade, Univ. Bordeaux, for valuable discussions.

References

[1] D.H. Waldeck, Chem. Rev. 91 (1991) 415.
[2] J. Saltiel, J. D'Agostino, E.D. Megarity, L. Metts, K.R. Neuberger, M. Wrighton, O.C. Zafiriou, Organic Photochemistry, vol. 3, in: O.L. Chapman (Ed.), Marcel Dekker, New York, 1971, Chapter 1, pp. 1.
[3] J. Saltiel, Y.-P. Sun, Photochromism – Molecules and Systems, in: H. Dürr, H. Bouas-Laurent (Eds.), Elsevier, Amsterdam, 1990, p. 64.
[4] J. Troe, Chem. Phys. Lett. 114 (1985) 241.
[5] P.M. Felker, A.H. Zewail, J. Phys. Chem. 89 (1985) 5402.
[6] G. Gershinsky, E. Pollak, J. Chem. Phys. 107 (1997) 812.
[7] J. Schroeder, D. Schwarzer, J. Troe, P. Vöhringer, Chem. Phys. Lett. 218 (1994) 43.
[8] W. Rettig, W. Majenz, R. Herter, J.F. Létard, R. Lapouyade, Pure Appl. Chem. 65 (1993) 1699.
[9] V. Bonacic-Koutecký, P. Bruckmann, P. Hiberty, J. Koutecký, C. Leforestier, L. Salem, Angew. Chem. Int. Ed. Engl. 14 (1975) 575.
[10] J. Michl, V. Bonacic-Koutecký, Electronic Aspects of Organic Photochemistry, Wiley, New York, 1990.
[11] W. Rettig, W. Majenz, Chem. Phys. Lett. 154 (1989) 335.
[12] P.R. Hammond, Opt. Commun. 29 (1979) 331.
[13] J.R. Taylor, Opt. Commun. 57 (1986) 117.
[14] V. Bonacic-Koutecký, J. Koutecký, J. Michl, Angew. Chem. Int. Edit. Engl. 26 (1987) 170.
[15] W. Rettig, W. Baumann, Photochemistry and Photophysics, vol. VI, in: J.F. Rabek (Ed.), CRC Press, Boca Raton, 1992, p. 79.
[16] W. Rettig, in: Topics in Current Chemistry, vol. 169, Electron Transfer I, J. Mattay (Ed.), Springer, Berlin, 1994, p. 253.
[17] W. Rettig, Ber. Bunsenges. Phys. Chem. 95 (1991) 259.
[18] C. Monte, K. Hoffmann, A. Siemoneit, M. Staak, P. Zimmermann, W. Rettig, R. Lapouyade, Fast Elementary Processes in Chemical and Biological Systems, in: A. Tramer (Ed.), American Institute of Physics conference proceedings 364, 1996, p. 47.
[19] E. Abraham, J. Oberlé, G. Jonusauskas, R. Lapouyade, C. Rullière, Chem. Phys. 214 (1997) 409.
[20] V. Papper, G. Likhtenshtein, D. Pines, E. Pines, Recent Research Development in Photochemistry and Photophysics, Transworld Research Network, 1998, in press.
[21] Z.R. Grabowski, K. Rotkiewicz, A. Siemiarczuk, D.J. Cowley, W. Baumann, Nouv. J. Chim. 3 (1979) 443.
[22] W. Rettig, Angew. Chem. Int. Edit. Engl. 25 (1986) 971.
[23] R. Lapouyade, K. Czeschka, W. Majenz, W. Rettig, E. Gilabert, C. Rullière, J. Phys. Chem. 96 (1992) 9643.
[24] V. Papper, D. Pines, G. Likhtenshtein, E. Pines, J. Photochem. Photobiol. A: Chem. 111 (1997) 87.
[25] H. Görner, J. Photochem. 19 (1982) 343.
[26] W.A. Yee, S.J. Hug, D.S. Kliger, J. Am. Chem. Soc. 110 (1988) 2164.
[27] M.T. Allen, D.G. Whitten, Chem. Rev. 89 (1989) 1691.
[28] J.B. Birks, D.J.S. Birch, Chem. Phys. Lett. 31 (1975) 608.
[29] P.C. Alford, T.F. Palmer, Chem. Phys. Lett. 127 (1986) 19.
[30] E.D. Cehelnik, R.B. Cundall, J.R. Lockwood, T.F. Palmer, J. Phys. Chem. 79 (1975) 1369.
[31] T. Itoh, B.E. Kohler, J. Phys. Chem. 91 (1987) 1760.
[32] D.-M. Shin, D.G. Whitten, J. Am. Chem. Soc. 110 (1988) 5206.
[33] U. Kopf, J. Heinze, Anal. Chem. 56 (1984) 1931.
[34] R.A. Velapoldi, M.S. Epstein, ACS Symp. Series 383 (1989) 98.
[35] T. Karstens, K.J. Kobs, Phys. Chem. 88 (1980) 1871.
[36] Principles and examples of the application of the method of singular value decomposition with respect to optical spectra ,in: E.R. Henry (Ed.), Biophys. J. 72 (1997) 652.
[37] E.R. Henry, J. Hofrichter, Methods Enzymol. 210 (1992) 129.
[38] M. Vogel, W. Rettig, Ber. Bunsenges. Chem. 91 (1987) 1241.
[39] AMPAC 5.0, © 1994 Semichem, 7128 Summit, Shawnee, KS 66216, USA.
[40] J. Del Bene, H.H. Jaffé, J. Chem. Phys. 48 (1968) 1807.
[41] J. Del Bene, H.H. Jaffé, J. Chem. Phys. 49 (1968) 1221.
[42] J. Del Bene, H.H. Jaffé, J. Chem. Phys. 50 (1969) 1126.
[43] Personal communication from D. Liotard, university of Bordeaux I, France, 1997.
[44] R. Schöneich, J. Bendig, D. Kreysig, Z. Naturforsch. 34a (1979) 1344.
[45] H.J. Kuhn, S.E. Braslavsky, R. Schmidt, Pure Appl. Chem. 61 (1989) 187.
[46] G. Zimmerman, L.-Y. Chow, U.-J. Paik, J. Am. Chem. Soc. 80 (1958) 3528.
[47] H. Mauser, Formale Kinetik, Bertelsmann Universitätsverlag, Düsseldorf 1974, p. 305.
[48] H. Gruen, H. Görner, Z. Naturforsch. 38A (1983) 928.
[49] W. Fuß, S. Lochbrunner, A.M. Müller, T. Schikarski, W.E. Schmid, S.A. Trushin, Chem. Phys. 232 (1998) 161.
[50] F. Bernardi, M. Olivucci, M.A. Robb, J. Photochem. Photobiol. A: Chem. 105 (1997) 365.
[51] J.-M. Viallet, F. Dupuy, R. Lapouyade, C. Rulliere, Chem. Phys. Lett. 222 (1994) 571.
[52] E. Abraham, J. Oberlé, G. Jonusauskas, R. Lapouyade, K. Minoshima, C. Rullière, Chem. Phys. 219 (1997) 73.
[53] W. Rettig, W. Majenz, R. Lapouyade, G. Haucke, J. Photochem. Photobiol. A: Chem. 62 (1992) 415.
[54] T.V. Singh, G.P. Pandey, K.N. Mehrota, Indian J. Chem., Sect. B 18 (1979) 8.
[55] S. Helm, J. Bendig, unpublished results.
[56] H. Mauser, Formale Kinetik, Bertelsmann-Universitätsverlag, Stuttgart, 1982.
[57] W. Rettig, V. Bonacic-Koutecký, Chem. Phys. Lett. 62 (1979) 115.